UDK 669.14.018.8:620.193
Original scientific article/Izvirni znanstveni članek

ISSN 1580-2949
MTAEC9, 44(2)67(2010)

INFLUENCE OF MnS INCLUSIONS ON THE CORROSION OF AUSTENITIC STAINLESS STEELS

VPLIV VKLJUČKOV MnS NA KOROZIJSKO ODPORNOST AVSTENITNIH NERJAVNIH JEKEL

Črtomir Donik, Irena Paulin, Monika Jenko

Institute of Metals and Technology, Lepi pot 11, SI-1000 Ljubljana, Slovenia
crtomir.donik@imt.si

Prejem rokopisa – received: 2009-09-19; sprejem za objavo – accepted for publication: 2009-12-21

The influence of alloy sulfur on the crevice solution chemistry and the nature of the surface in the crevice during initiation were investigated. Two austenitic steels with different amounts of sulfur in the alloy, AISI 316L and SS 2343, were compared using electrochemical measurements with an additional standard test – ASTM G48. The electrochemical measurements, i.e., a potentiodynamic measurement, a linear polarization and a Tafel polarization, were performed in a typical corrosion solution of 3.5 % NaCl and 0.1 % NaCl. The results show the difference for the steels in a low concentration of Cl^- ions, while in the higher concentration of the Cl^- ions the steels act very similarly. The MnS inclusions were analyzed and characterized using high-resolution SEM with EDX elemental analyses. The SE images show large differences for these materials in terms of the amount of inclusions. From the EDX measurements it was confirmed that the inclusions consist of Mn and S, and very few other types of inclusions were found.

Keywords: corrosion, stainless steel, MnS inclusion, electrochemical corrosion tests, ASTM G48

Raziskovali smo vpliv vsebnosti žvepla na korozijske lastnosti dveh avstenitnih nerjavnih jekel. Z elektrokemijskimi meritvami in s standardnimi preizkusi jamičaste korozije ASTM G48 smo poskušali ugotoviti razlike med dvema preiskovanima materialoma. Preiskovali smo dve po sestavi podobni nerjavni jekli tipa AISI 316L in SS 2343 z različnima vsebnostma žvepla. Elektrokemijske meritve: potenciodinamske meritve, linearne polarizacije in Tafelove polarizacije, smo naredili v tipični raztopini za korozijske preizkuse 3,5 % in 0,1 % NaCl. Pri nizkih koncentracijah kloridnih ionov v raztopini lahko opazimo odmike med lastnostmi materialov, medtem ko prihaja pri visokih koncentracijah kloridnih ionov do tega, da imata materiala zelo podobne korozijske lastnosti. S pregledom pod vrstičnim elektronskim mikroskopom visoke ločljivosti z EDX analizatorjem smo določili obliko in vrsto vključkov ter njihovo sestavo. Pri SEM-posnetkih lahko opazimo razlike med materialoma po količini vključkov in potrdimo z EDX-analizo, da vključki vsebujejo elementa Mn in S ter da skoraj ni prisotnih drugih vključkov.

Ključne besede: korozija, nerjavna jekla, MnS-vključki, elektrokemijski korozijski preizkusi, ASTM G48

1 INTRODUCTION

The effect of sulfur on the corrosion behavior of austenitic stainless steel is manifested through the behavior of the sulfide inclusions due to the low solubility of sulfur in ferrous metals.[1–5] Sulfide inclusions have been recognized as preferential sites for localized corrosion for almost 100 years, for steels, and for almost 60 years for stainless steels.[1,6–13] The effect of an alloying element can be manifested through effects on the passive film, the local solution chemistry, or the interfacial electrochemical kinetics.[10,14–23] The effects of alloyed sulfur on the localized corrosion in steels have been ascribed by various workers to each of these mechanisms. In our stainless steel, SS 2343, the sulfur is added to enhance lubrication through inclusions in the oil-free processes.[2,22–24]

Many theories have proposed that changes in the occluded chemistry are the key due to the effects of the dissolution products of the MnS inclusions.[2,23] Because most dissolved sulfur species have been observed to enhance metal dissolution, many sulfur species (i.e., sulfate, thiosulfate, elemental sulfur, and aqueous sulfide) have been predicted to result from MnS inclusion dissolution in the occluded region. Two categories of sulfur species may be considered, depending on the origin of the species: (a) sulfur species in the environment (H_2S, HS^-, S_2O_3, SO_2, HSO_4^-, SO_4^{2-}) and (b) sulfur in the material (sulfur in solid solution, sulfur segregated at the surface or in the grain boundaries, and sulfur in the sulfide inclusions).[4,25] In the case of the MnS sulfate inclusions, although their determination effect on the corrosion of steel and stainless steel has been extensively studied, the exact mechanism is not known. Sulfate (SO_4^{2-}) was predicted by Eklund to be the dominant dissolved sulfur species originating from sulfide inclusions via the electrochemical oxidation of the metal sulfide in the inclusions to sulfate, with the simultaneous formation of acid.[26]

The alteration of the chemistry of the stainless-steel surface in the vicinity of the sulfide inclusions, and the subsequent effects on the interfacial kinetics, has also been proposed as playing an important role in localized corrosion initiation. It was also observed that the corrosion initiated primarily at the inclusion edges, and concluded that the bare metal initially exposed upon inclusion dissolution became passivated and did not

corrode until the precipitation of a $MnCl_2$ salt film (found using AES) occurred to restrict the mass transport. Smialowska[27] proposed that localized corrosion initiated by the formation of a thick salt layer at weak spots in the passive film (such as might be expected at inclusions), followed by hydrolysis of the salt leading to local acidification, inclusion dissolution and exposure of the bare, unprotected metal. Marcus et al.[27] proposed that regardless of its origin (i.e., from the alloy or from the solution), sulfur enhances metal dissolution via the formation of an adsorbed sulfur layer, which leads to weakening of the metal-metal bonds on the surface, thereby reducing the activation energy barrier for metal dissolution.

The important aspect of the corrosion is the formation of the passive film on the top of stainless steels. After the formation of this passive film on the bare metal surface, a slow dissolution of the metal cations continues, involving dissolution at the passive film surface and transport of the ions through the oxide. The question then arises as to where the bulk impurities (e.g., sulfur) go during the process. Above the critical concentration of sulfur at the interface (metal/oxide) the breakdown of the passive film was observed.[4]

There is much evidence for the damaging effect of the sulfur species over a wide range of corrosion-related service failures. The relation between the sulfur-induced corrosion mechanism presented in areas of practical importance can be rationalized on the basis of (a) the source of the sulfur, (b) the transport process to the metal surface, and (c) the condition of the reduction of the sulfur species into the harmful chemical state of sulfur.

Although it is clear that sulfide inclusions act as preferential sites for localized corrosion, the mechanism by which this occurs has remained unclear.

In the present work two stainless steels with different amounts of sulfur in the alloy were studied. The study was conducted using different electrochemical techniques: potentiodynamic measurements, linear polarization and Tafel polarization. MnS inclusions were investigated using SEM with EDX measurements.[28,29]

2 EXPERIMENTAL

Two types of stainless steel were investigated. Their compositions were confirmed using an Optical Emission Spectrometer (OES) as follows (weight percent): 17.0 % Cr, 10.0 % Ni, 1.5 % Mn, 0.40 % Si, 0.035 % P, 0.002 % S, 0.015 % C and the remainder Fe, denoted as AISI 316L; and 16.5 % Cr, 10.5 % Ni, 1.5 % Mn, 0.38 % Si, 0.041 % P, 0.025 % S, 0.020 % C and the remainder Fe, denoted as SS 2343.

The experiments for the electrochemical measurements were carried out in 3.5 % sodium chloride solution with and without 0.5-M Na_2S, and in 0.1 % sodium chloride solution. The standard test ASTM G48 was performed in a 6 % $FeCl_3$ solution at room temperature. All the chemicals were from Merck, Darmstadt, Germany.

The test specimens were cut into discs of 15 mm diameter. The specimens were abraded with SiC emery paper down to a 1000-grit prior to the electrochemical measurements. The specimens were then embedded in a Teflon PAR holder and employed as a working electrode. The reference electrode was a saturated calomel electrode (SCE, 0.242 V vs. SHE) and the counter electrode was a high-purity graphite rod.

Tafel polarization, potentiodynamic and linear polarization measurements were recorded using an EG&G PAR PC-controlled potentiostat/galvanostat Model 263 with SoftCorr computer programs. In the case of the potentiodynamic measurements and the linear polarization the specimens were immersed in the solution 1 h prior to the measurement in order to stabilize the surface at the open-circuit potential. Potentiodynamic curves were recorded starting at 250 mV more negative than the open-circuit potential. The potential was then increased, using a scan rate of 1 mV s^{-1}, until the transpassive region was reached. Linear polarization curves were recorded at ±10 mV around the open-circuit potential using a scan rate of 0.1 mV s^{-1}. The Tafel polarization curves were recorded at ±250 mV around the open-circuit potential using a scan rate of 0.5 mV s^{-1}. Some of the samples were passivated in 3M HNO_3 for 30 min to prevent localized corrosion on the boldly exposed surfaces.

The surface analytical experiments were performed using a high-resolution Scanning Electron Microscope JEOL JSM-6500F.

The standard test method ASTM G 48 for the pitting corrosion resistance of stainless steels and related alloys uses ferritic chloride solution. The method is used to compare the resistance of the stainless steels and related alloys in order to increase the resistance to pitting and crevice-corrosion initiation under the specific conditions. In our experiments *Method A* of standard ASTM G48 – ferric chloride pitting test was used: 6.0 % $FeCl_{3(aq)}$ with test specimens of 25 mm × 50 mm without sharp edges. All the specimens in the test had the same dimensions and were grinded with silicon grinding paper 600. The samples were weighed before and after exposure, and exposed to the solution for 72 h.

3 RESULTS AND DISCUSSION

3.1 Polarization measurements

In order to study the influence of the sulfur inclusions in stainless steels, different test solutions were used. The linear polarization curves were recorded for both materials on samples around the corrosion potential (**Figure 1**).

The calculations were performed from linear polarization measurements using the equation:

$$R_p = \beta_a \beta_c / (2.3\ I_{corr} (\beta_a + \beta_c)).$$

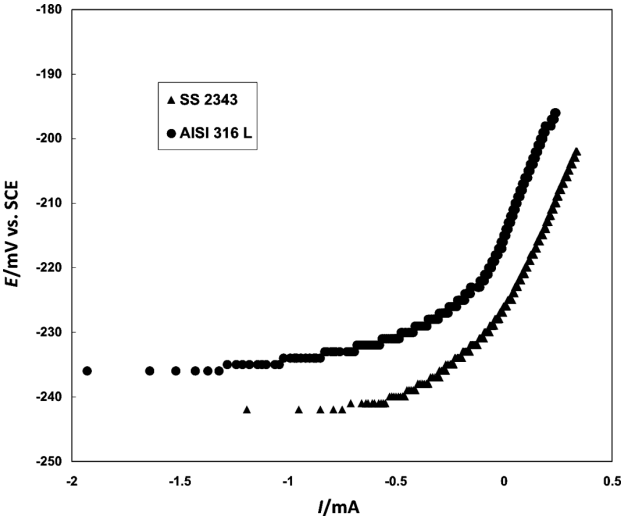

Figure 1: Linear polarization curves of the stainless steels AISI 316 L and SS 2343 in a 0.1 % NaCl solution

Slika 1: Graf linearne polarizacije nerjavnih jekel AISI 316 L in SS 2343 v 0,1 % raztopini NaCl

The polarization resistance, R_p, is evaluated from the linear polarization curves by applying a linear least-squares fit of the data around ±10 mV E_{corr}. The corrosion current, $I_{corr.}$, is calculated from R_p, the least-squares slope, and the Tafel constants, β_a and β_c, of 100 mV decade^{-1}. The value of $E(I = 0)$ is calculated from the least-squares intercept.

The corrosion rate was calculated by using the following conversion formula: $v_{corr.} = C(EW/d)(I_{corr.}/A)$, where EW is the equivalent weight of the sample in g, A is the sample area in cm^2, d is its density in g/mL, and C is a conversion constant that is dependent upon the units desired. The slopes of both materials were similar, so the corrosion rates of these materials did not differ significantly from each other. The corrosion potential for the stainless-steel AISI 316 L was –220 mV and for SS 2343 it was –230 mV.

The potentiodynamic curves were measured in two different solutions: 0.1% and 3.5 % NaCl, with and without the addition of $Na_2S{\cdot}9H_2O$. **Figure 2** shows the potentiodynamic curves of the stainless steels AISI 316 L and SS 2343 in 0.1 % NaCl without any pre-passivation of the materials. After 1 h of stabilization at the open-circuit potential, the corrosion potentials (E_{corr}) for both materials were around –350 mV. Following the Tafel region both alloys exhibited passive behavior. The passive region is limited by the breakdown potential (E_b), which corresponds to the oxidation of water and the transpassive oxidation of the metal species. The breakdown potential for SS 2343 was approximately 380 mV and for AISI 316L it was 600 mV.

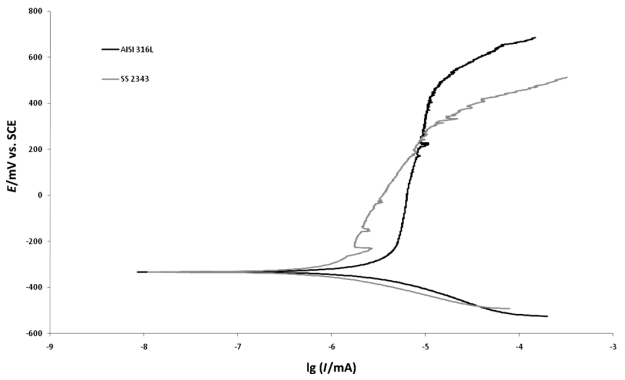

Figure 2: Potentiodynamic curves of the stainless steels AISI 316 L and SS 2343 passivated samples in a 0.1 % NaCl solution

Slika 2: Potenciodinamski krivulji pasiviranih vzorcev nerjavnih jekel AISI 316 L in SS 2343 v 0,1-odstotni raztopini NaCl

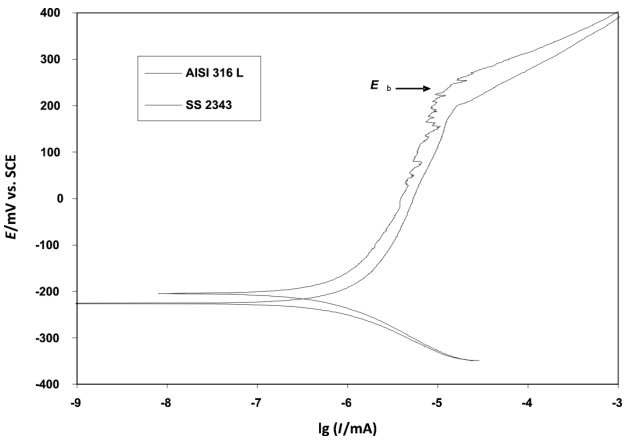

Figure 3: Potentiodynamic curves of the stainless steels AISI 316 L and SS 2343 in a 3.5 % NaCl solution

Slika 3: Potenciodinamski krivulji vzorcev nerjavnih jekel AISI 316 L in SS 2343 v 3,5-odstotni raztopini NaCl

Figure 3 shows the potentiodynamic curves of the stainless steels AISI 316L and SS 2343 in 3.5 % NaCl. After 1 h of stabilization at the open circuit, the potential values of E_{corr} for both alloys were around –200 mV, although it was slightly higher for AISI 316L. The values of E_b are similar for both steels and are around 200 mV and 250 mV for SS 2343 and AISI 316L,

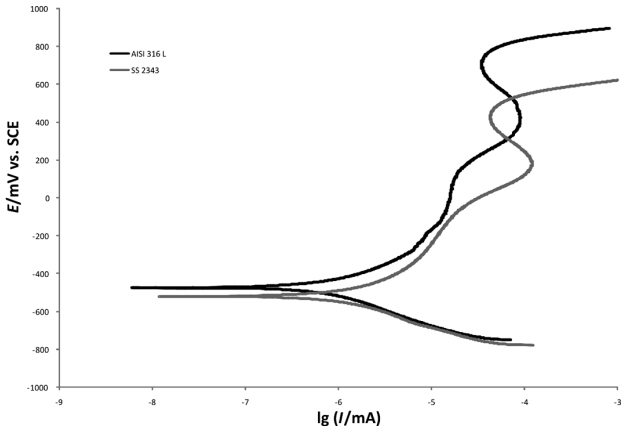

Figure 4: Potentiodynamic curves of the stainless steels AISI 316 L and SS 2343 in 0.1 % NaCl and 0.5-M Na_2S solution

Slika 4: Potenciodinamski krivulji nepasiviranih vzorcev nerjavnih jekel AISI 316 L in SS 2343 v 0,1-odstotni raztopini NaCl v 0,5 M Na_2S

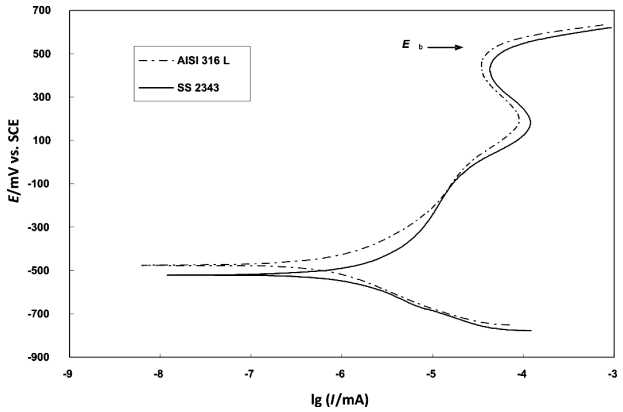

Figure 5: Potentiodynamic curves of the stainless steels AISI 316 L and SS 2343 in 3.5 % NaCl and 0.5-M Na_2S solution
Slika 5: Potenciodinamski krivulji nepasiviranih vzorcev nerjavnih jekel AISI 316 L in SS 2343 v 3,5-odstotni raztopini NaCl v 0,5 M Na_2S

respectively. The breakdown potentials for these alloys are relatively low due to a narrowing of the passive region in the presence of a high concentration of the Cl^- ions. As a result, the corrosion current values are relatively high, and therefore the corrosion rates are around mm per year (**Table 1**).

Table 1: Corrosion rates calculated from R_p for the stainless steels AISI 316 L and SS 2343 in (10^{-3} mm per year)
Tabela 1: Korozijske hitrosti, izračunane iz R_p, za nerjavni jekli AISI 316 L in SS 2343 v (10^{-3} mm na leto)

Material	$v_{corr.}$ (10^{-3} mm/y)	
	NaCl	NaCl+Na_2S
AISI 316 L	140.6	46.75
SS 2343	158.9	53.93

The results mentioned above suggest that the distinction between the selected materials should be investigated in a low concentration of Cl^- ions. Therefore, the corrosive activator 0.5M Na_2S was added to the solution and the corrosion characteristics were measured. The pH of the test solution evidently increased; therefore, the corrosion potential was moved to more negative values to approximately –500 mV (**Figures 4 and 5**), whereas the corrosion current and the corrosion rate do not increase significantly (Table 1). In the presence of S^{2-} ions both steels exhibited better corrosion characteristics. However, we have to take into account that the pH is evidently higher than in the case of the test solution without the addition of the sulfide and that at approximately pH 12 the stainless steels are in a highly passivated area. In the 0.1 % solution of NaCl, both steels

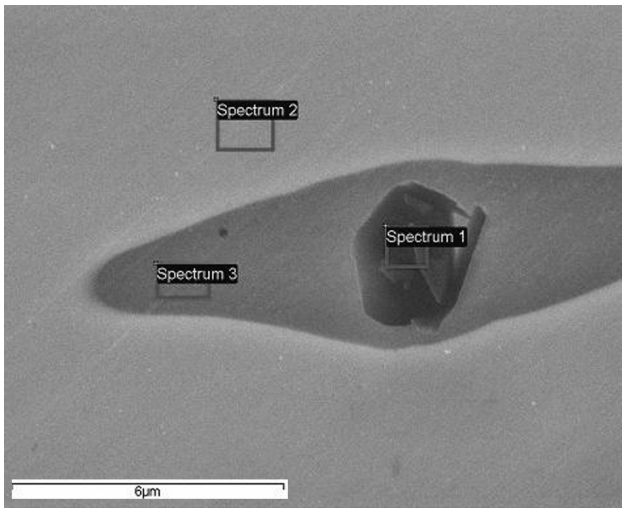

Figure 6: SE image of an inclusion in the sample SS 2343 with the areas of the EDX measurements
Slika 6: SE-posnetek površine vzorca s področij EDX-analize

differed significantly, the passive region was evidently wider for the AISI 316 L compared to the SS 2343 (**Figure 2**). With the addition of 0.5-M Na_2S the values of E_{corr} were shifted from approximately –350 mV to –500 mV and –550 mV for the AISI 316L and SS 2343, respectively (**Figure 4**). The extension of the passive region increased with the addition of the sulfide. The E_b values were shifted to 450 mV and 750 mV for the AISI 316L and SS 2343, respectively (**Figure 4**).

3.2 Scanning Electron Microscopy

Figure 6 shows a SE image of an inclusion on the surface of the SS 2343; the EDX analysis was also performed on the marked areas. The results are shown in **Table 2**. The EDX measurements inside the inclusion showed the increased amount of Mn and S, with an atomic ratio 1 : 1, which indicates the presence of MnS in the inclusion (Spectrum 1 and 3). Spectrum 2 was performed on the bulk material and its composition confirmed the chemical composition of the standard composition of this type of stainless steel.

3.3 Standard corrosion test

Standard corrosion test for the pitting corrosion resistance of stainless steels and related alloys in the ferritic chloride solution, ASTM G 48, was performed for both alloys. The results are shown in **Table 3**, where the weight loss is shown in absolute mass and also in

Table 2: EDX measurements of the inclusion in SS 2343 in weight percent
Tabela 2: EDX-meritve vključka na površini jekla SS 2343 v masnih deležih (%)

	C	O	Mg	Al	S	Ti	Cr	Mn	Fe	Ni
Spectrum 1		27.31	1.08	24.34	14.40	0.82	4.66	21.59	3.82	1.98
Spectrum 2	2.25	0.67					16.67	1.77	64.37	10.82
Spectrum 3					29.60		5.68	50.09	4.15	1.30

mass percentage. The results show a slight difference in the weight loss, which could be the result of an increased amount of sulfur manganese inclusions. This small increase in the weight loss for the sample with the higher amount of sulfur inclusions is in the range of the measurement uncertainty and it could also be correlated to either a lower corrosion characteristic of the metal or a difference in the preparation of the samples.

Table 3: Results for ASTM G 48 test
Tabela 3: Rezultati preizkusa ASTM G 48

	m_1/g	m_2/g	Δm/g	Δm/%
AISI 316 L	3.0098	2.9195	0.0903	3.0
SS 2343	3.1527	2.9959	0.1568	4.9

4 CONCLUSION

The materials AISI 316 L and SS 2343 are chemically almost identical; the only difference is in the amount of sulfur, which is up to 10 times higher in the SS 2343. The results from the electrochemical measurements show a slight difference in the corrosion characteristics in favor of the AISI 316 L. However, the distinction between the selected materials is possible only in the solution containing low Cl^- concentrations. In contrast, in the presence of high Cl^- concentrations, the test solution is so aggressive that the difference in the chemical composition of both materials is diminished. The Na_2S addition in the corrosion solutions increased the pH to around pH 12, and therefore pushed the stainless steel into the passive region so the S^{2-} ions did not play an important role in the differentiation of these to stainless steels. The difference between both materials is expressed by a standard corrosion test, ASTM G 48, where the AISI 316L showed a slightly better corrosion characteristic than the SS 2343 stainless steel.

5 REFERENCES

[1] Brossia, C. S.; Kelly, R. G., Occluded solution chemistry control and the role of alloy sulfur on the initiation of crevice corrosion in type 304ss. Corrosion Science 40 (**1998**) 11, 1851–1871

[2] Krawiec, H.; Vignal, V.; Heintz, O.; Oltra, R.; Chauveau, E., Dissolution of chromium-enriched inclusions and pitting corrosion of resulfurized stainless steels. Metallurgical and Materials Transactions a-Physical Metallurgy and Materials Science 37A (**2006**) 5, 1541–1549

[3] Krawiec, H.; Vignal, V.; Heintz, O.; Oltra, R., Influence of the dissolution of MnS inclusions under free corrosion and potentiostatic conditions on the composition of passive films and the electrochemical behaviour of stainless steels. Electrochimica Acta 51 (**2006**) 16, 3235–3243

[4] Sulfur-Assisted Corrosion Mechanisms and the Role of Alloyed Elements. In Corrosion Mechanisms in Theory and Practice, Marcus, P., Ed. CRC Press: 2002

[5] Schmuki, P.; Hildebrand, H.; Friedrich, A.; Virtanen, S., The composition of the boundary region of MnS inclusions in stainless steel and its relevance in triggering pitting corrosion. Corrosion Science 47 (**2005**) 5, 1239–1250

[6] Brossia, C. S.; Kelly, R. G., Influence of alloy sulfur content and bulk electrolyte composition on crevice corrosion initiation of austenitic stainless steel. Corrosion 54 (**1998**) 2, 145–154

[7] Donik, C.; Kocijan, A.; Mandrino, D.; Paulin, I.; Jenko, M.; Pihlar, B., Initial oxidation of duplex stainless steel. Applied Surface Science 255 (**2009**) 15, 7056–7061

[8] Kocijan, A.; Milosev, I.; Pihlar, B., The influence of complexing agent and proteins on the corrosion of stainless steels and their metal components. Journal of Materials Science-Materials in Medicine 14 (**2003**) 1, 69–77

[9] Kocijan, A.; Milosev, I.; Merl, D. K.; Pihlar, B., Electrochemical study of Co-based alloys in simulated physiological solution. Journal of Applied Electrochemistry 34 (**2004**) 5, 517–524

[10] Kocijan, A.; Donik, C.; Jenko, M., Electrochemical and XPS studies of the passive film formed on stainless steels in borate buffer and chloride solutions. Corrosion Science 49 (**2007**) 5, 2083–2098

[11] Jenko, M.; Mandrino, D., Application of surface analytical technique HRAES to metallurgy. Strojarstvo 41 (**1999**) 3–4, 107–110

[12] Mandrino, D.; Vrbanic, D.; Jenko, M.; Mihailovic, D.; Pejovnik, S., AES and XPS investigations of molybdenum-sulfur-iodine-based nanowire-type material. Surface and Interface Analysis 40 (**2008**) 9, 1289–1293

[13] Donik, C.; Kocijan, A.; Paulin, I.; Jenko, M., Oxidation of duplex stainless steel at moderately elevated temperature. Materiali in tehnologije / Materials and technology 2009, In Press, Corrected Proof

[14] Abreu, C. M.; Cristóbal, M. J.; Losada, R.; Nóvoa, X. R.; Pena, G.; Pérez, M. C., Comparative study of passive films of different stainless steels developed on alkaline medium. Electrochimica Acta 49 (**2004**) 17–18, 3049–3056

[15] Gojic, M.; Marijan, D.; Kosec, L., Electrochemical behavior of duplex stainless steel in borate buffer solution. Corrosion 56 (**2000**) 8, 839–848

[16] Kocijan, A.; Milosev, I.; Pihlar, B., Cobalt-based alloys for orthopaedic applications studied by electrochemical and XPS analysis. Journal of Materials Science-Materials in Medicine 15 (**2004**) 6, 643–650

[17] Kocijan, A.; Donik, C.; Jenko, M., The corrosion behaviour of duplex stainless steel in chloride solutions studied by XPS. Materiali in Tehnologije 43 (**2009**) 4, 195–199

[18] Kocijan, A.; Donik, C.; Jenko, M., The electrochemical study of duplex stainless steel in chloride solutions. Materiali in Tehnologije 43 (**2009**) 1, 39–42

[19] Olefjord, I.; Clayton, C. R., Surface-composition of stainless-steel during active dissolution and passivation. Isij International 31 (**1991**) 2, 134–141

[20] Olsson, C. O. A.; Landolt, D., Passive films on stainless steels - chemistry, structure and growth. Electrochimica Acta 48 (**2003**) 9, 1093–1104

[21] Stypula, B.; Stoch, J., The characterization of passive films on chromium electrodes by XPS. Corrosion Science 36 (**1994**) 12, 2159–2167

[22] Bastos, I. N.; Tavares, S. S. M.; Dalard, F.; Nogueira, R. P., Effect of microstructure on corrosion behavior of superduplex stainless steel at critical environment conditions. Scripta Materialia 57 (**2007**) 10, 913–916

[23] Wranglen, G., Pitting and sulfide inclusions in steel. Corrosion Science 14 (**1974**) 5, 331–349

[24] Yin, Z. F.; Zhao, W. Z.; Tian, W.; Feng, Y. R.; Yin, C. X., Pitting behavior on super 13Cr stainless steel in 3.5% NaCl solution in the presence of acetic acid. Journal of Solid State Electrochemistry 13 (**2009**) 8, 1291–1296

[25] Marcus, P.; Talah, H., The sulfur-induced breakdown of the passive film and pitting studied on nickel and nickel-alloys. Corrosion Science 29 (**1989**) 4, 455–463

[26] Eklund, G. S., Initiation of pitting at sulfide inclusions in stainless-steel. Journal of the Electrochemical Society 121 (**1974**) 4, 467–473

[27] Lukac, C.; Lumsden, J. B.; Smialowska, S.; Staehle, R. W., Effects of temperature on kinetics of passive film growth on iron. Journal of the Electrochemical Society 122 (**1975**) 12, 1571–1579

[28] Mandrino, D.; Godec, M.; Torkar, M.; Jenko, M., Study of oxide protective layers on stainless steel by AES, EDS and XPS. Surface and Interface Analysis 40 (**2008**) 3–4, 285–289

[29] Paulin, I.; Donik, C.; Jenko, M., Mechanisms of HF bonding in dry scrubber in aluminium electrolysis. Materiali in Tehnologije 43 (**2009**) 4, 189–193

[30] International, A., ASTM G48-03(2009) Standard Test Methods for Pitting and Crevice Corrosion Resistance of Stainless Steels and Related Alloys by Use of Ferric Chloride Solution.